



HAL
open science

Cell cycle features of primate embryonic stem cells.

Anne-Catherine Fluckiger, Guillaume Marcy, Mélanie Marchand, Didier Negre, Cosset François-Loïc, Shoukhrat Mitalipov, Don Wolf, Pierre Savatier, Colette Dehay

► To cite this version:

Anne-Catherine Fluckiger, Guillaume Marcy, Mélanie Marchand, Didier Negre, Cosset François-Loïc, et al.. Cell cycle features of primate embryonic stem cells.. Stem cells (Dayton, Ohio), 2006, 24, pp.547-56. 10.1634/stemcells.2005-0194 . inserm-00132737v2

HAL Id: inserm-00132737

<https://inserm.hal.science/inserm-00132737v2>

Submitted on 26 Feb 2007

HAL is a multi-disciplinary open access archive for the deposit and dissemination of scientific research documents, whether they are published or not. The documents may come from teaching and research institutions in France or abroad, or from public or private research centers.

L'archive ouverte pluridisciplinaire **HAL**, est destinée au dépôt et à la diffusion de documents scientifiques de niveau recherche, publiés ou non, émanant des établissements d'enseignement et de recherche français ou étrangers, des laboratoires publics ou privés.

Cell-cycle features of primate embryonic stem cells

Anne-Catherine Fluckiger^{1,2,*}, Guillaume Marcy^{1,2,*}, Mélanie Marchand^{1,2}, Didier Nègre^{3,4,5}, François-Loïc Cosset^{3,4,5}, Shoukhrat Mitalipov⁶, Don Wolf⁶, Pierre Savatier^{1,2,7,§} and Colette Dehay^{1,2,7,§}.

(1) INSERM, U371, Cerveau et Vision, Department of Stem Cells and Cortical Development, 18 avenue Doyen Lépine, 69500 Bron, France.

(2) Université Claude Bernard Lyon I, IFR19 Institut Fédératif des Neurosciences, 69500 Bron, France.

(3) INSERM, U412, 69007 Lyon, France.

(4) Ecole Normale Supérieure de Lyon, 69007 Lyon, France.

(5) Université Claude Bernard Lyon I, IFR128 BioSciences Lyon-Gerland, 69007 Lyon, France.

(6) Oregon National Primate Research Center, Oregon Health & Science University, 505 NW 185th Avenue, Beaverton, OR 97006.

(7) INSERM, U371, PrimaStem, 69500 Bron, France.

* the first two authors have equally contributed to this work

§ corresponding authors : savatier@lyon.inserm.fr - dehay@lyon.inserm.fr

Running title : Cell-cycle control of primate ES cells

Keywords : Rhesus ES cells, cell-cycle, stemness

ABSTRACT

Using flow cytometry measurements combined with quantitative analysis of cell-cycle kinetics, we show that rhesus monkey ES cells are characterised by an extremely rapid transit through the G1 phase which accounts for 15% of the total cell-cycle duration. Monkey ES cells exhibit a non phasic expression of cyclin E which is detected during all phases of the cell-cycle and do not growth-arrest in G1 following γ -irradiation, reflecting the absence of a G1 checkpoint. Serum deprivation or pharmacological inhibition of Mitogen Activated Protein Kinase Kinase (MEK) did not result in any alteration in the cell-cycle distribution, indicating that ES cell growth does not rely on mitogenic signals transduced by the Ras/Raf/MEK pathway. Taken together, these data indicate that rhesus monkey ES cells, like their murine counterparts, exhibit unusual cell-cycle features in which cell-cycle control mechanisms operating during the G1 phase are reduced or absent.

INTRODUCTION

There is accumulating evidence that cell-cycle control in mouse embryonic stem (ES) and somatic cells differs in that the mouse ES cell-cycle is not dependent on a functional p16^{ink4a}/cyclin D:Cyclin-dependent kinase (Cdk)4/pRB:E2F pathway [1-5]. Rather, the cyclin E:Cdk2 and cyclin A:Cdk2 complexes in ES cells are constitutively active throughout the cell-cycle suggesting that the mitotic cycle is constitutively primed for DNA replication [6]. Interestingly, mouse ES cells have a very short G1 phase of approximately 1.5 hr and they predominantly express the hyperphosphorylated form of the retinoblastoma protein (pRB) (specific of the S and G2/M phases of the cell-cycle) [7], indicating that newly formed cells can enter a new phase of DNA replication very shortly after exit from mitosis. Another striking feature of the mitotic cycle of mouse ES cells is the lack of dependency on serum stimulation [8] and Mitogen Activated Protein Kinase Kinase (MEK)-associated signalling [4,9,10]. Mouse ES cells rely on Phosphatidyl Inositol-3 kinase (PI3K)-dependent signalling for progression through the G1 phase [10] as well as for inhibition of differentiation [11]. However, PI3K activity is not dependent on persistent serum stimulation [10], but rather largely relies both on stimulation of the Leukemia Inhibitory Factor (LIF) receptor and on expression of the ES cell-specific Eras factor [12]. In addition, mouse ES cells do not undergo cell-cycle arrest at the G1 checkpoint in response to DNA damage or nucleotide depletion [13,14], although they synthesize abundant quantities of transcriptionally active p53 [13]. Taken together, these findings indicate that the mitotic cycle of ES cells largely escapes from external mitogenic stimuli and instead relies largely on intrinsic factors.

A crucial question is whether the unusual cell-cycle characteristics of mouse ES cells are shared by primate ES cells. Here, we show that rhesus monkey ES cells display most of the cell-cycle characteristics of mouse ES cells, including shortening of G1 phase, non-phasic

expression of cyclin E, predominance of hyperphosphorylated RB, lack of dependency on serum stimulation and MEK signalling, and absence of a DNA damage checkpoint in G1. We thus propose that these unique cell-cycle characteristics are critical, and possibly universal features of ES cells.

MATERIAL AND METHODS

Rhesus monkey ES cell culture.

Procedures for rhesus ES cell line ORMES-1 and ORMES-6 culture have been described previously [15]. Briefly, ORMES ES cells were grown at 37°C in 5% CO₂ atmosphere on mitotically inactivated mouse embryonic fibroblasts (MEF) feeder cells in Dulbecco's Modified Eagle's Medium (DMEM) (Invitrogen) supplemented with 20% foetal bovine serum (FBS) (Hyclone), 0.1 mM β-mercaptoethanol (Sigma), 1% nonessential amino acids (Invitrogen), and 2 mM L-glutamine (Invitrogen). ES cell colonies were passaged every 4-5 days by treatment with 1 mg/ml collagenase IV (20-30 mins at 37°C), followed by mechanical dissociation.

PD98059 and U0126 (Sigma) were dissolved in dimethylsulfoxide (Sigma) and added to the medium at a concentration of 25 μM and 10 μM, respectively.

Lentiviral vector production and infection of ES cells.

R4SA-EFs-EGFP-W, a Simian Immunodeficiency Virus-based vector, harbors the sequence encoding the enhanced Green Fluorescent Protein (eGFP) driven by the minimal version of the human EF1α promoter (EFs). It was generated by replacing the ClaI/XhoI restriction fragment containing the CMV-GFP cassette in pSIV-gaMES4 [16] by a ClaI/Sall restriction fragment containing the EFs-EGFP cassette (a gift from Patrick Salmon). The method for

producing SIV-based vectors in 293T cells is fully described elsewhere [17,18]. Briefly, 293T cells were transfected with a mixture of DNAs containing 10 µg of the *pGRev* plasmid encoding the VSV-G envelope, 10 µg of *pSIV3⁺* plasmid encoding the gag, pol, tat and rev proteins, and 13 µg of the *R4SA-EFs-EGFP-W* plasmid, using the calcium phosphate precipitation technique. The following day, cells were refed with 7 ml of DMEM and further cultured for 24 hours. The supernatant was then collected, cleared by centrifugation (3,000 RPM, 15 min) and passed through a 0.8 µm filter. Prior to infection, ORMES-1 cells were treated with 1mg/ml collagenase IV for 3-5 min at 37°C. Clumps of undifferentiated ORMES-1 cells were isolated by mechanical dissociation and transferred to fresh medium (500 µl) containing SIV-eGFP. Cells were incubated for 4 hrs at 37°C, before being replated on fresh feeder cells.

Time-Lapse Videomicroscopy recording of cell division.

ORMES-1 cells were grown in a 5% CO₂ atmosphere at 37°C for 4-5 days in a Pecon incubating chamber placed on a Leica DMIRBE inverted microscope stage. Observations of individual eGFP⁺ cells were made with an 10x objective under halogen illumination. Twenty fields were scanned per coverslip per hour using Metamorph software. Subsequent analysis of the movies allowed estimation of the cell-cycle length of individual eGFP⁺ cells as measured by the time elapsed between two successive mitosis [19].

Cell-cycle kinetics measurements.

S phase and G1+G2+M phase durations can be derived from Bromodeoxyuridine (BrdUrd) cumulative labeling experiments [20-22]. Cumulative BrdUrd labeling was performed on ORMES cells grown on coverslips in 24-well plates in standard conditions. Forty-eight hrs after plating, BrdUrd (20 µg/ml) was added to the medium for the indicated times. Cells were

fixed with 2% paraformaldehyde (PFA) and the labeling index (LI) values determined (proportion of BrdUrd⁺ cells, *i.e.* cells that were in S phase during BrdUrd exposure, with respect to the undifferentiated pool, *i.e.* the Oct-4⁺ cell population). Percentage of labelled mitosis (PLM) labeling [21-23] was used to determine the G2/M duration. Forty-eight hrs after plating, cultures were pulse-labelled for 1 hr with BrdUrd (20 µg/ml). For both procedures, three independent experiments were performed with the ORMES-1 cell line and two experiments with ORMES-6. Each time point was repeated on two sister coverlips. After survival periods, cultures were fixed in 2% PFA and processed for the detection of BrdUrd incorporation and Oct-4 expression. Cells were counterstained with Hoechst 33258 for 3 min to allow the identification of mitotic figures.

In situ immunofluorescence.

ORMES cells were fixed in 2% PFA in phosphate-buffered saline (PBS) at 4°C for 1 hr. Immunohistochemistry was performed by a two-step procedure. Cells were permeabilized in Tris Buffer Saline (TBS) + 0.2% Triton X-100, 0.1% Tween-20, for 20 min. Non-specific binding was blocked with 10% normal goat serum (Jackson ImmunoResearch Laboratories) for 1 hr at RT. To detect Oct-4 protein, cells were first incubated for 1 hr at 30°C with mouse monoclonal antibody anti-Oct-4 (C-10: sc5279) from Santa-Cruz biotechnology (1:1000 in DAKO-diluent). Cyclin E and Cyclin A were detected using C-19 (sc-198) and H-432 (sc-751) respectively antibodies (1/100, Santa Cruz Biotechnology) incubated overnight at 4°C. Ki-67 was detected using phycoerythrine-conjugated anti-human Ki-67 monoclonal antibody (BD Bioscience, ref. 36525). After three rinses in TBS, cells were exposed either to affinity-purified goat anti-mouse or goat anti-rabbit IgG conjugated either to indocarbocyanine or to cyanin (respectively Cy3 and Cy2, Jackson ImmunoResearch Laboratories) for 1 hr at RT followed by nuclear staining with 1ng/ml Hoechst 33258 for 3 min. After three rinses in TBS,

coverslips were mounted on slides. To detect both Oct-4 expression and BrdU incorporation, cells were first treated to reveal Oct-4 expression as described above. DNA was then denatured by incubation in 2N HCl, followed by a wash in a borate buffer, pH 8.5. Non-specific binding was blocked with 10% normal goat serum. BrdU incorporation was revealed by incubation with Alexa 488-conjugate anti-BrdU antibody (1:50 in DAKO-diluent) (Molecular Probes) for 2 hours at RT. Nuclei were counterstained with Hoechst 33258. Coverslips were examined using an oil objective microscope under UV light to detect FITC (filter 450-490 nm), indocarbocyanine 3 (filter 550-570 nm) and Hoechst 33258 (filter 355-425 nm). Coverslips were scanned at regular spacing with a grid corresponding to a field of 0.128 mm². 100 to 150 fields were observed per coverslip. Immunopositive cells were plotted onto a chart using the Mercator software (Explora Nova).

Flow cytometric analysis of cell cycle distribution.

Single cell suspensions of ORMES cells were obtained by treatment with 1 mg/ml collagenase IV (37°C for 20-30 min) followed by treatment with 0.1% trypsin (37°C for 3 min). For DNA content analysis, cells were fixed in 70% ethanol, rehydrated in PBS, treated for 30 min with RNase A (1 mg/ml) and for 5 min with propidium iodide (1µg/ml). Fluorescence intensity was determined by flow cytometry on a Becton Dickinson FACscan equipped with a 488 nm argon laser. Data acquisition was performed with the CellQuest (Becton Dickinson) software, and the percentages of G1-, S-, and G2-phase cells were calculated with the MODFIT-LT software program (Verity Software House Inc). To discriminate proliferating ORMES-1 cells from non-proliferating feeder cells, cultures were exposed to BrdUdR (20 µg/ml) for 24 hrs. Fresh medium containing BrdUdR was changed every 12 hrs. Colonies were then dispersed into a single cell suspension, fixed in 70% ethanol and rehydrated in PBS. DNA denaturation was subsequently performed by incubation in 2N

HCl followed by three washes in PBS containing 0.5% Tween and 0.5% BSA (PBT). Cells were then incubated with FITC-conjugated anti-BrdU monoclonal antibody (BD Bioscience, 1:50 in PBT) for 30 min at RT in the dark. After extensive washes in PBT, cells were incubated with 1 mg/ml RNase (20 min, RT) followed by propidium iodide treatment (1 μ g/ml) and analysed as indicated above.

Western blotting.

Cells were lysed in 20 mM Hepes pH 7.4, 100 mM NaCl, 50 mM NaF, 1% Triton X-100, 10% glycerol, 1 mM dithiothreitol, 1 mM sodium orthovanadate, 1 mM phenylmethylsulfonyl fluoride and a cocktail of protease inhibitors (Roche) for 1 hour at 4°C. Protein lysates were then cleared by centrifugation (14,000 RPM for 20 min). Total proteins (30 μ g) were electrophoresed on 10% SDS-polyacrylamide gel and electroblotted onto nitrocellulose membranes. For analysis of pRB expression, 2×10^6 cells were lysed in 100 μ l of 60 mM Tris-HCl pH 6.8, 1.25% SDS, 175 mM 2-Mercaptoethanol. Samples (30 μ l) were analysed on 5% SDS polyacrylamide gel. After overnight treatment with blocking buffer (50 mM Tris-Hcl pH 7.6, 150 mM NaCl, 5% dry milk), the membranes were probed with anti-cyclin E (Sigma C4976), anti-cyclin A (Santa Cruz sc-751), or anti-pRB monoclonal antibodies (BD Bioscience, ref. 554136). Blots were incubated with horseradish peroxidase-coupled anti-mouse, or anti-rabbit IgG and developed using ECL reagents (Amersham).

RESULTS

Population doubling time and cell-cycle duration of the ORMES-1 ES cells.

ORMES-1 cells were grown on mitotically inactivated MEF feeder cells in the presence of 20% FBS [15]. They were routinely seeded at a 0.3×10^5 cells/cm² cell density. Daily counts of cell numbers showed an initial moderate increase for the first three days (average doubling time of approximately 70 hrs) (Figure 1A). Counts returned an average doubling time of approximately 25 hrs during day 4 and 5. A negative binomial regression test performed in the R statistical computing environment (R Development Core Team, 2004) [24] revealed that there is a statistical difference in the growth rate between the 0-3 days period and the 4-5 days period ($p < 0.05$ for both growth curves), as indicated by the abrupt change in the slope of the growth curves at day 3. At day 6 and 7, cells reached confluency and population growth slowed most likely as a consequence of cell death and higher rates of spontaneous differentiation.

To determine whether the variations in growth rates were paralleled by changes in the expression of pluripotency markers, colonies were immunolabelled to detect expression of the Oct-4 transcription factor (Figure 1B, C). At day 1, 69 +/- 22% (n = 14) of cells within colonies expressed Oct-4. This percentage peaked at 99 +/- 1% (n = 10) at day 3, to decline to 80 +/- 30% (n = 10) at day 6. Therefore, all subsequent experiments were carried out on ORMES cells between day 3 and 5 which corresponds to the optimal growth phase, when 99% of cells express the pluripotency marker Oct-4. Within the ORMES colonies, 99 +/- 1% of Oct-4⁺ cells were cycling cells, as shown by double immunolabelling against Ki-67 and Oct-4 (Figure 1D).

Doubling-time is a crude measure of proliferation rates and is contaminated with cell death and spontaneous differentiation. In order to accurately measure the mitotic cycle

duration, we performed time-lapse videomicroscopy analysis on individual ORMES-1 cells. Cells were infected with SIV-eGFP -a SIV-based lentiviral vector expressing the Enhanced Green Fluorescent Protein (eGFP)- at a multiplicity of infection of 100 virus/cell so as to transduce the *eGFP* gene into approximately 2-3% of the cell population. Infected cells were propagated for one month and weekly checked for expression of eGFP by fluorescent microscopy. The fraction of eGFP-expressing cells did not vary with time indicating identical rates of growth for infected and non-infected cells (data not shown).

Cells were grown on inactivated MEF. 4 days after replating, the proliferative behavior of individual eGFP⁺ cells was recorded by time-lapse videomicroscopy during a 48hrs period. The time between two successive mitosis was calculated for 32 individual cells. As shown in Figure 2, the cell-cycle duration of individual ORMES-1 ranges from 12 to 21 hrs (median value is 15 hrs).

ORMES-1 ES cell have an unusual cell cycle distribution.

Next, we examined the distribution of ORMES-1 cells in cell-cycle phases using single colour flow cytometry analysis after DNA staining with propidium iodide (PI). Cells were harvested at day 4 of the culture, corresponding to the maximum growth rate (Figure 1A). To rule out a putative bias due to the presence of growth-inactivated MEF, cultures were first incubated for 24 hours with 50 μ M BrdUrd in order to label all proliferating cells. Subsequent analysis of DNA content stained with PI was restricted to the BrdUrd⁺ cells (Figure 3A,B). Under these conditions, the fractions of G1, S and G2/M phase cells were 16 +/- 3%, 56 +/- 3%, and 28 +/- 5% respectively. ORMES-1 cells were induced to differentiate by withdrawal of MEF and culture on gelatine-coated dishes for 1 week. Under these conditions, the fractions of G1, S and G2/M phase cells were 45 +/- 2%, 29 +/- 6%, and 26 +/- 5% respectively (Figure 3C). Therefore, differentiation of ORMES-1 cells is accompanied by dramatic changes in the cell-

cycle distribution, characterized by a large increase in the proportion of cells in G1 phase and a decrease in the proportion of cells in S phase.

Duration of individual phases of the cell cycle of ORMES-1 and ORMES-6 cells.

We investigated the duration of the individual phases of the cell cycle in undifferentiated, self-renewing ORMES-1 and ORMES-6 cells, by combining the BrdUrd cumulative labeling technique [19,20] with computation of the percentage of labeled mitosis (PLM) [22, 23]. BrdUrd cumulative labeling is based on continuous BrdUrd exposure that leads to the incorporation of BrdUrd by successive cohorts of cycling cells progressing through S phase. The proportion of cells labeled by the BrdUrd exposure (LI) is monitored at regular intervals throughout the duration of T_C - T_S . In this system, prolonged exposure to BrdUrd for periods equal to T_C - T_S returns LI values of 100% [21]. $T_{G1+G2+M}$ is determined by projecting the extrapolated 100% LI value onto the x -axis. Projection on the negative limb of the x -axis determinates T_S . So as to monitor the cell-cycle of undifferentiated cells, and to exclude spontaneously differentiating cells from the calculation, the LI was computed within the Oct4⁺ cell population (LI was calculated as the proportion of Oct4⁺ that were labeled with BrdUrd). Three independent BrdUrd cumulative labelling experiments were performed on ORMES-1 cells (Figure 4A). Cumulative BrdUrd labeling returned T_C values ranging from 16 (blue curve) to 20 hrs (green curve). T_S , and $T_{G1+G2+M}$ values were comprised between 8 (blue curve) and 10 hrs (green curve). One experiment of cumulative BrdUrd labeling in ORMES-6 cells (black curve) returned T_C , T_S , and $T_{G1+G2+M}$ values of 17, 7 and 10 hrs, respectively.

So as to estimate the duration of G2/M, the PLM method was implemented on sister cultures of the four independent experiments. Following a 1 hr exposure to BrdUrd, the time interval required for 100% labeling of mitotic figures corresponds to the passage through G2 and M (Figure 4B). So as to restrict the analysis to undifferentiated, self-renewing ORMES

cells, the percentage of BrdUrd labelled mitotic figures was calculated within the Oct-4⁺ population. In ORMES-1 cells, this analytical procedure returned maximum values for G2/M of 9 (blue curve) to 10 hrs (green curve). When T values are subtracted from T_{G1+G2/M} values of the same experiment, this indicates that T_{G1} is reduced, ranging from a few minutes (blue and green curves) to 1 hr (red curve). In ORMES-6 cells, the PLM method indicates that maximum value of T_{G2/M} is 7 hrs, returning a T_{G1} of 3 hrs (Figure 4B). These results show that the relative duration of G1 phase with respect to T_C is comprised between 10 and 20% in ORMES – as shown in the FACS profile (Figure 3B).

DNA damage checkpoints in ORMES-1 cells.

To determine whether ORMES-1 cells have intact cell-cycle response to DNA damage, we analysed the effects of γ -irradiation on the cell cycle. In somatic cells, DNA damage results in rapid decrease in the S-phase population, due to p53- and Cdc25A-dependent mechanisms that prevent G1 cells with DNA damage from entering S phase [25-27]. As shown in Figure 5, the G1-phase fraction in ES cells harvested 3 to 18 hours after exposure to 6 Grays (Gy) ionizing radiation decreased from 22 +/- 0.1% to 7 +/- 0.5%. In contrast, the G2-phase fraction increased from 36 +/- 1% to 70 +/- 2%. These results indicate that ORMES-1 ES cells do not have a functional DNA-damage-response pathway for growth-arrest in G1. By contrast, they exhibit growth-arrest in the G2 phase. Note that the fraction of cells in the G1 phase in the non-irradiated cell population (22%) was larger than the fraction of G1 cells found in the ES cell population analyzed in Figure 3B (16%) The presence of feeder cells in the irradiation experiment largely accounts for this difference as the vast majority of feeder cells were in G1 (data not shown).

Elevated levels of cyclins A and E throughout the cell cycle in ORMES-1 cells.

We investigated cyclin E and cyclin A expression by immunoblot analysis. Undifferentiated ORMES-1 cells expressed high levels of cyclin A and E and these levels decreased dramatically after differentiation induced by low density culture in feeder-free conditions for 5 days (Figure 6A). To determine if cyclin E and cyclin A levels fluctuate during cell-cycle progression as observed in somatic cells or, alternatively, if their expression is not cell-cycle dependent like in mouse ES cells [6], cyclin E and cyclin A were analysed by *in situ* immunofluorescence in the ORMES-1 cell population. 97 +/- 2% and 78 +/- 4% of Oct4⁺ ORMES-1 cells expressed cyclin E and cyclin A, respectively (Figure 6B,C). By contrast, only a small fraction of differentiated Oct4⁻ ORMES cells expressed cyclin E (6 +/- 5%) and cyclin A (22 +/- 5%) (Figure 6B,D). Together, these data show that cyclin E is expressed throughout the cell-cycle in ORMES-1 cells indicating that its expression is not cell-cycle dependent. By contrast, not all Oct4⁺ ORMES-1 cells expressed cyclin A, suggesting that cyclin A expression is down-regulated in a sub-fraction of undifferentiated ORMES-1 cells.

Predominance of hyperphosphorylated pRB in ORMES-1 cells.

In parallel, phosphorylation of the retinoblastoma gene product (pRB) was investigated by immunoblot analysis. Mostly hyperphosphorylated pRB – specific of the S, G2 and M phases of the cell-cycle - was detected in undifferentiated ORMES-1 cells, whereas hypophosphorylated, G1-specific, pRB was predominant in differentiated cells (Figure 6E). The predominance of hyperphosphorylated pRB in ORMES-1 cells reflects the cell-cycle distribution of undifferentiated cells in which S and G2/M phases represent approximately 85% of the total cell cycle.

Dependency on serum stimulation and MEK signaling for G1/S transition in ORMES-1 cells.

We next addressed the question of whether rhesus monkey ES cells were dependent on persistent serum stimulation for progression in the cell-cycle. Following serum deprivation for 24 hrs - a duration sufficient for every cell of the population to pass at least once through any serum checkpoint - we failed to detect any alteration in the cell-cycle distribution of ORMES-1 cells (X^2 test, $p > 0.5$), as shown by flow cytometry analysis (Figure 7A). Pairwise comparisons between control and serum-deprived sister cultures did not reveal significant variations in the percentages of cells in G1 ($p = 0.5$), in S ($p = 0.92$), and in G2/M ($p = 0.89$) (Student T-test, 3 experiments) (Figure 7B).

Treatment of ORMES-1 cells for 24 hrs with 25 μ M PD98059, or with 10 μ M U0126, to specifically inhibit MEK activity [28,29] did not result in any significant alteration in the cell-cycle distribution (PD9805-treated versus control cells : X^2 test, $p > 0.5$; U0126-treated versus control cells : X^2 test, $p > 0.5$) (Figure 7C). Pairwise comparisons between control and PD98059-treated sister cultures did not reveal significant variations in the percentages of cells in G1 ($p = 0.3$), in S ($p = 0.4$), and in G2/M ($p = 0.6$) (Student T-test, 3 experiments). Pairwise comparisons between control and U0126-treated sister cultures did not reveal significant variations in the percentages of cells in G1 ($p = 0.35$), in S ($p = 0.56$), and in G2/M ($p = 0.71$) (Student T-test, 3 experiments) (Figure 7D).

To confirm that MEK inhibition did not result in long term alteration of the growth rate, ORMES-1 cells were propagated in the presence of PD98059, or with vehicle alone, for 7 days. Daily counts of cell numbers did not reveal difference in growth rates between PD-treated and control cells (Figure 7E). Taken together these data indicate that ORMES-1 cells

do not require persistent mitogenic stimulation and functional MEK signaling to progress through the G1/S transition.

DISCUSSION

These results indicate that there are important similarities between murine and primate ES cell-cycle characteristics. Like their murine counterpart, rhesus monkey ES cells show a reduced G1 phase, a predominance of hyperphosphorylated RB, an absence of DNA-damage checkpoint in G1, non cell-cycle dependent expression of cyclin E, and lack of dependency on persistent serum stimulation and active MEK signaling during cell-cycle progression.

Using the BrdUrd cumulative labelling technique, we estimated that the total cell-cycle duration of ORMES-1 cells was 20 hours. This technique, when applied to heterogeneous cell populations cycling at different rates, returns predominantly the cell-cycle duration of the slowest cycling cells [20]. Time-lapse videomicroscopy was therefore used to provide the range of the cell-cycle duration values of individual ORMES-1 cells. This revealed that the population of ORMES-1 cells is heterogeneous with cells progressing through a complete cell-cycle in a time-window ranging from 12 to 21 hrs. The reason why ORMES-1 cells are heterogeneous in their cell-cycle duration is unclear. It is unlikely to result from mutations which would heritably influence the cell-cycle duration since careful examination of the cell-cycle durations of mother and daughter cells failed to reveal any positive correlation (data not shown). Interestingly, examination of the position of eGFP-expressing mother and daughter cells revealed extensive movements within the colony. These movements are likely to modify the microenvironment such as the accessibility of ES cells to extracellular matrix-associated cytokines provided by feeder cells. This could result in randomly influencing the cell-cycle duration of individual ES cells.

The most striking feature of the murine ES cell cycle, apart from it being unusually rapid, is a short G1 phase which represents approximately 15% of the total cell-cycle duration, or 2 hrs. The duration of the G1 phase of mouse ES cells was calculated by measuring the delay between release from mitotic block and onset of [³H]-thymidine incorporation in synchronized cells [7]. Conditions for propagating primate ES cells precluded large-scale amplification which would be necessary to synchronize them by mitotic block. Therefore, we used an indirect method based on the combination of cumulative BrdUrd labelling and PLM to calculate the durations of the individual phases of the cell-cycle in asynchronously growing cell populations. Despite monkey ES cells having a total cell-cycle duration up to twice as long as that of mouse ES cells, the relative duration of the G1 phase is similar in the two species. In both species, the hyperphosphorylated form of pRB is predominant [7], further indicating that the vast majority of the cells are in the S and the G2/M phases of the cell-cycle. Taken together, these results indicate that a short G1-phase duration might be a common, and possibly universal, characteristic of ES cells, reflecting unique mechanisms of cell-cycle control which have been conserved throughout vertebrate evolution. Cells of the embryonal carcinoma (EC) stem cell line P19 also display a unusually short G1 phase [30]. Pluripotent EC stem cells that can be induced to differentiate into mesodermal derivatives following treatment with retinoic acid (RA). Interestingly, upon synchronization by exposure to the reversible mitotic blocker, P19 EC cells were particularly vulnerable to RA while they progressed from mitosis to the next S-phase and, by contrast, became resistant to RA-induced differentiation when they reached S-phase [30]. These observations suggest that the G1 phase corresponds to a window of increased sensitivity to differentiation signals. It is thus tempting to speculate that shortening of G1 phase might shield pluripotent cells from activities that induce differentiation [22].

HAL author manuscript inserm-00132737, version 2

Which mechanism, therefore, underlies the rapid transit through the G1 phase in monkey ES cells? In mouse ES cells, there is compelling evidence that the G1 → S transition is not dependent on a functional cyclin D:Cdk4/6 → RB:E2F pathway [1-5] and that rapid progression through the cell-cycle largely, if not exclusively, relies on constitutively active cyclin E:Cdk2 and cyclin A:Cdk2 complexes [6]. Monkey ES cells also express cyclin E during all phases of the cell-cycle suggesting that ectopic cyclin E-Cdk2 kinase activity may also be a characteristic feature of primate ES cells. Interestingly, ORMES-1 cells did not express cyclin A in all phases of their cell-cycle, as opposed to mouse ES cells [6]. Thus, mouse and monkey ES cells are likely to differ on the basis of the cell-cycle dependent regulation of cyclin A. The heterogeneous cell-cycle duration that characterizes rhesus ES cells could result from discontinuous expression of cyclin A in a subset, or in all, Oct4⁺ cells.

Mouse ES cells fail to undergo cell-cycle arrest in the G1 phase in response to DNA damage [13]. Both mechanisms involved in DNA-damage-dependent cell-cycle arrest – the chk1/chk2 kinase-dependent degradation of the Cdc25A phosphatase [27] and the activation of the p53-p21 axis [31] – are not functional in mouse ES cells [14]. Here, we show that rhesus monkey ES cells are similarly impaired in their ability to respond to growth-arrest in G1 after treatment with ionizing radiation. Then the question arises as to how these cells maintain genomic integrity in the absence of a G1 checkpoint. Following DNA-damage both mouse and rhesus ES cells undergo apoptosis ([13] and our unpublished data), suggesting that the function of p53 in ES cells is to trigger apoptosis in order to efficiently eliminate cells with damaged DNA. An alternative mechanism was recently suggested in mouse ES cells where, following DNA damage, transcriptionally active p53 repressed the activity of the *nanog* promoter and irreversibly induced differentiation, thus eliminating DNA-damaged cells from the pool of undifferentiated stem cells [32]. Whether a similar mechanism operates in primate ES cells remains to be determined.

We show that rhesus monkey ES cells, like their murine counterpart [8, 10], do not rely on persistent serum stimulation for cell-cycle progression. Noteworthy, serum was withdrawn for 24 hours, thus allowing all cells to progress through any serum-dependent checkpoint, regardless of their position in the cell-cycle at the onset of serum withdrawal. These data indicate that rhesus monkey ES cells can efficiently progress through the G1 to S phase transition in the absence of mitogenic signals. Rhesus monkey ES cells also appear not sensitive to pharmacological inhibition of MEK, a property shared with mouse ES cells [10, 33, 34]. In the mouse, inhibition of MEK-dependent signalling facilitates self-renewal [33] by sustaining expression of the expression of Oct-4 [34]. It remains to be determined whether a similar mechanism operates in primate ES cells.

CONCLUSIONS

To conclude, our results show that rhesus monkey ES cells share several fundamental properties of the cell cycle with mouse ES cells. We propose that these unique properties, that are distinct from that of other mammalian non-transformed cell types, are fundamental characteristics of embryonic stem cells. In view of the present results, together with several reports pointing to common mechanisms in cell-cycle regulation of mouse ES cells and other pluripotent cell types such as the pluripotent cells of the mouse epiblast [35], the epiblast-like (EPL) cells [6], the P19 EC cells [36,37], and the embryonic germ (EG) cells [38], we hypothesize that these unique cell cycle characteristics of ES cells may contribute to stemness.

ACKNOWLEDGEMENTS

We are grateful to Véronique Cortay for assistance in the immunohistochemical techniques, to Florence Wianny for expert help with the cell cultures, and to Ken Knoblauch for assistance in the statistical analyses. We are indebted to Henry Kennedy for advice and constant support as well as for critical reading of the manuscript. This work was supported by Région Rhône-Alpes (Emergence, N° 0101681601 “Thématique prioritaire cellules souches”, N° 0301455301), Association Française contre la Myopathie (INSERM/AFM N° 4CS016F), INSERM AVENIR 2002 programm. ACF is supported by an INSERM postdoctoral grant.

LEGENDS

Figure 1 : Population doubling time and expression of Oct-4 and Ki67 markers in ORMES-1 cells. ORMES cells were plated on inactivated MEF at a density of 0.3×10^5 cells per cm^2 . (A) Cell numbers were counted at each time point (2 to 3 replicates) in two independent experiments using a Trypan blue exclusion assay. Means and standard errors to the mean (SEM) are indicated on the graph. (B) Immunohistofluorescent detection of Oct-4 (revealed by Cy3) in undifferentiated ORMES-1 cells between day 1 and day 6 of culture. Curve represents the mean percentages of Oct-4⁺ cells within colonies (n = 7 to 14) of ORMES-1 cells. (C) Immunohistofluorescent detection of Oct-4 (revealed by Cy3) in ORMES-1 cells at day 2, 4 and 6 of the culture (D) Immunohistofluorescent detection of Oct-4 (revealed by Cy2) and Ki-67 (revealed by phycoerythrine) in ORMES-1 cells at day 3 of the culture. (C,D) Bar = 10 μM .

Figure 2 : Cell-cycle duration of individual ORMES-1 cells measured by time lapse videomicroscopy two passages after infection with lentiviral vector expressing eGFP. Histogram represents the duration of 32 individual cell divisions over a time period of 48 hrs.

Figure 3 : Cell-cycle distribution of ORMES-1 cells as measured by flow cytometry. ORMES-1 cells were grown in the presence of 50 μM BrdUrd for 24 hrs to label all proliferating cells. Cells were then processed for detection of BrdUrd incorporation and analysis of DNA content. (A) Dot plot representation of DNA/BrdUrd biparametric analysis for ORMES-1 and inactivated MEF. DNA was stained with propidium iodide (PI) (x-axis) and BrdUrd (y-axis) was revealed with FITC-conjugated anti-BrdUrd. (B) Histogram representation of the cell-cycle distribution of ORMES-1 cells gated as the BrdUrd⁺ cell

population (gate R1). (C) Histogram representation of the cell-cycle distribution of ORMES-1 after differentiation induced by withdrawal of MEF and culture on gelatine-coated dishes for 1 week. (B,C) Histograms show one representative experiment. Values are means and SEM calculated from three independent replicates. Frequencies of cells in each phase of the cell-cycle were calculated using MODFIT software.

Figure 4 : Duration of individual phases of the ORMES-1 and ORMES-6 cell-cycle by means of cumulative BrdUrd incorporation and Percentage of Labelled Mitosis (PLM) techniques. (A) Determination of T_c (length of the total cell-cycle), T_s (length of the S-phase) and $T_{G1+G2+M}$ (length of the G1+G2+M phases) by cumulative BrdUrd incorporation. ORMES-1 and ORMES-6 cells were plated at a density of 0.3×10^5 cells per cm^2 . Three days after plating, cells were refed with fresh medium containing $50 \mu M$ BrdUrd, further cultured for 1 to 10 hours, then processed at regular time intervals for dual detection of Oct-4 expression and BrdUrd incorporation. The four curves correspond to the percentages of $BrdUrd^+/Oct4^+$ cells (labelling indices, LI) calculated in four independent experiments [three experiments carried on ORMES-1 (red, green and blue curves), and one experiment carried out on ORMES-6 (black curve)]. For each curve, values are means and SEM calculated from 3 replicates (replicates are sister coverslips from which individual LI are calculated). Projection of the extrapolated 100% LI value on the x -axis returns the duration of G1+G2+M phases ($T_{G1+G2+M}$). Projection on the negative limb of the axis returns the duration of the S-phase (T_s). (B) Determination of $T_{G2/M}$ (length of G2/M) by the PLM technique. ORMES-1 and ORMES-6 cells were plated at a density of 0.3×10^5 cells per cm^2 . Three days after plating, cells were exposed to $50 \mu M$ BrdUrd for 1 hr and further cultured for 1 to 10 hrs in BrdU-free medium. At regular time intervals, cells were processed for dual detection of Oct-4 expression and BrdUrd incorporation. The curves indicates the percentages of $BrdUrd^+/Oct4^+$ mitosis in

four independent experiments [three experiments on ORMES-1 (red, green and blue curves), and one experiment on ORMES-6 (black curve)]. For each curve, values are means and SEM calculated from 2-3 replicates (replicates are sister coverslips from which individual percentages are calculated). Projection of the extrapolated 100% value on the x -axis returns the duration of (T_{G2+M}). The G1 duration has been calculated by subtraction of T_{G2+M} from $T_{G1+G2/M}$ using values obtained from sister cultures, which values are indicated in the same color code (*i.e.* the red curves in A and in B come from sister cultures).

Figure 5 : DNA damage checkpoints in ORMES-1 cells. ORMES-1 cells were plated at a density of 0.3×10^5 cells per cm^2 on MEF. Three days after plating, cells were irradiated (6 Gy) and further cultured for 3 to 18 hrs before being processed for analysis of DNA content by flow cytometry. (A) Cell-cycle distributions of irradiated ORMES-1 cells as measured 0 to 24 hrs after irradiation. (B) Percentages of ORMES-1 cells in G1, S and G2/M phases of the cell-cycle as a function of time following irradiation (means and SEM were calculated from three independent experiments). Percentages were calculated using MODFIT software.

Figure 6 : Expression of cyclin E, cyclin A, and pRB in ORMES-1 cells. (A) Western blot analysis of the steady-state levels of cyclin E and cyclin A in undifferentiated ORMES-1 cells (1) and in their differentiated derivatives (2). Differentiation was achieved by plating ORMES-1 cells at high density on feeder-free, gelatin-coated culture dishes for 5 days, with reduced serum (5%). (B) Percentages of cyclin E and cyclin A positive cells in Oct-4⁺ ES cells and Oct-4⁻ ES-derived cells calculated after immunohistofluorescence. 2 coverslips were examined for both cyclin E and cyclin A expression. The percentage of cyclin E⁺ cells was estimated on 590 Oct-4⁺ cells and 848 Oct-4⁻ cells. A total of 580 Oct-4⁺ cells and 1123 Oct-4⁻ cells were counted to determine the percentage of cells expressing cyclin A expression. ***

: $p < 0.001$ (Student T-test). (C) Immunohistofluorescent detection of Oct-4 (revealed by Cy2) and cyclin E (revealed by Cy3) in undifferentiated ORMES-1 cells (panel 1) or in differentiated ORMES-1 cells (panel 2). (D) Immunohistofluorescent detection of Oct-4 (revealed by Cy2) and cyclin A (revealed by Cy3) in undifferentiated ORMES-1 cells (panel 1) or in differentiated ORMES-1 cells (panel 2). Western blot analysis of pRB expression in undifferentiated ORMES-1 ES cells (1), in embryonic fibroblasts (2). p105 and p110 indicate molecular weights of hypophosphorylated and hyperphosphorylated pRB, respectively. (C,D) Bar = 10 μ M.

Figure 7 : Dependency on serum stimulation and MEK signaling of ORMES-1 cells. ORMES-1 cells were plated at a density of 0.3×10^5 cells per cm^2 . (A-D) Two days after plating, cells were refed with fresh medium lacking serum, or containing the MEK inhibitors PD98059 (PD98) or U0126, or vehicle (DMSO) alone, and further cultured for 24 hrs. Cells were then processed for DNA analysis by flow cytometry. Percentages of cells in each phase of the cell-cycle were calculated using MODFIT software. (A) Cell-cycle distribution of ORMES-1 cells cultured in the presence (+ FBS) or in the absence (-FBS) of serum (one representative experiment). Distributions are compared by means of χ^2 test. (B) Histograms showing the percentages of ORMES-1 cells in G1, S and G2/M phases (+/- FBS). Means and SEM were calculated from three independent experiments and compared by means of Student T-test. ns, non significant. (C) Cell-cycle distribution of ORMES-1 cells cultured in the presence of 25 μ M PD98059, or 10 μ M U0126, or in vehicle alone (one representative experiment). Distributions are compared by means of χ^2 test. (D) Histograms showing the percentages of ORMES-1 cells in G1, S and G2/M phases (+/- MEK inhibitors). Means and SEM were calculated from three independent experiments and compared by means of Student T-test. ns, non significant. (E) ORMES-1 cells were propagated in the presence of PD98059

(dotted line), or in vehicle alone (plain line), for 7 days. Cell numbers were counted at the indicated time points using a Trypan blue exclusion assay. Means and SEM were calculated from two replicates.

REFERENCES

1. Savatier P, Lapillonne H, van Grunsven LA et al. Withdrawal of differentiation inhibitory activity/leukemia inhibitory factor up-regulates D-type cyclins and cyclin-dependent kinase inhibitors in mouse embryonic stem cells. *Oncogene* 1996;12:309-322.
2. Dannenberg JH, van Rossum A, Schuijff L et al. Ablation of the retinoblastoma gene family deregulates G(1) control causing immortalization and increased cell turnover under growth-restricting conditions. *Genes Dev* 2000;14:3051-3064.
3. Sage J, Mulligan GJ, Attardi LD et al. Targeted disruption of the three Rb-related genes leads to loss of G(1) control and immortalization. *Genes Dev* 2000;14:3037-3050.
4. Burdon T, Smith A, Savatier P. Signalling, cell cycle and pluripotency in embryonic stem cells. *Trends Cell Biol* 2002;12:432.
5. White J, Stead E, Faast R et al. Developmental Activation of the Rb-E2F Pathway and Establishment of Cell Cycle Regulated Cdk Activity During Embryonic Stem Cell Differentiation. *Mol Biol Cell* 2005;16:2018-2027.
6. Stead E, White J, Faast R et al. Pluripotent cell division cycles are driven by ectopic Cdk2, cyclin A/E and E2F activities. *Oncogene* 2002;21:8320-8333.
7. Savatier P, Huang S, Szekely L et al. Contrasting patterns of retinoblastoma protein expression in mouse embryonic stem cells and embryonic fibroblasts. *Oncogene* 1994;9:809-818.

8. Schrott G, Weinhold B, Lundberg AS et al. Serum response factor is required for immediate-early gene activation yet is dispensable for proliferation of embryonic stem cells. *Mol Cell Biol* 2001;21:2933-2943.
9. Burdon T, Stracey C, Chambers I et al. Suppression of SHP-2 and ERK signalling promotes self-renewal of mouse embryonic stem cells. *Dev Biol* 1999;210:30-43.
10. Jirmanova L, Afanassieff M, Gobert-Gosse S et al. Differential contributions of ERK and PI3-kinase to the regulation of cyclin D1 expression and to the control of the G1/S transition in mouse embryonic stem cells. *Oncogene* 2002;21:5515-5528.
11. Paling NR, Wheadon H, Bone HK et al. Regulation of embryonic stem cell self-renewal by phosphoinositide 3-kinase-dependent signalling. *J Biol Chem* 2004;279:48063-48070.
12. Takahashi K, Mitsui K, Yamanaka S. Role of ERas in promoting tumour-like properties in mouse embryonic stem cells. *Nature* 2003;423:541-545.
13. Aladjem MI, Spike BT, Rodewald LW et al. ES cells do not activate p53-dependent stress responses and undergo p53-independent apoptosis in response to DNA damage. *Curr Biol*. 1998;8:145-155.
14. Hong Y, Stambrook PJ. Restoration of an absent G1 arrest and protection from apoptosis in embryonic stem cells after ionizing radiation. *Proc Natl Acad Sci U S A* 2004;101:14443-14448.
15. Mitalipov SM, Kuo HC, Hennebold JD et al. Oct-4 expression in pluripotent cells of the rhesus monkey. *Biol Reprod* 2003;69:1785-1792.
16. Mangeot PE, Duperrier K, Negre D et al. High levels of transduction of human dendritic cells with optimized SIV vectors. *Mol Ther* 2002;5:283-290.

17. Negre D, Mangeot PE, Duisit G et al. Characterization of novel safe lentiviral vectors derived from simian immunodeficiency virus (SIVmac251) that efficiently transduce mature human dendritic cells. *Gene Ther* 2000;7:1613-1623.
18. Mangeot PE, Negre D, Dubois B et al. Development of minimal lentivirus vectors derived from simian immunodeficiency virus (SIVmac251) and their use for gene transfer into human dendritic cells. *J Virol* 2000;74:8307-8315.
19. Lukaszewicz A, Savatier P, Cortay V et al. Contrasting effects of basic fibroblast growth factor and neurotrophin 3 on cell cycle kinetics of mouse cortical stem cells. *J Neurosci* 2002;22:6610-6622.
20. Nowakowski RS, Lewin SB, Miller MW. Bromodeoxyuridine immunohistochemical determination of the lengths of the cell cycle and the DNA-synthetic phase for an anatomically defined population. *J Neurocytol* 1989;18:311-318.
21. Dehay C, Savatier P, Cortay V et al. Cell-cycle kinetics of neocortical precursors are influenced by embryonic thalamic axons. *J Neurosci* 2001;21:201-214.
22. Lukaszewicz A, Savatier P, Cortay V et al. G1 phase regulation, area-specific cell cycle control, and cytoarchitectonics in the primate cortex. *Neuron* 2005;47:353-364.
23. Quastler H, Sherman FG. Cell population kinetics in the intestinal epithelium of the mouse. *Exp Cell Res* 1959;17:420-438.
24. R Development Core team. A language and environment for statistical computing. R Foundation for Statistical Computing, Vienna, Austria. ISBN 3-900051-07-0, URL <http://www.R-project.org>. 2004.
25. Kastan MB, Onyekwere O, Sidransky D et al. Participation of p53 protein in the cellular response to DNA damage. *Cancer Res* 1991;51:6304-6311.

26. Di Leonardo A, Linke SP, Clarkin K et al. DNA damage triggers a prolonged p53-dependent G1 arrest and long-term induction of Cip1 in normal human fibroblasts. *Genes Dev* 1994;8:2540-2551.
27. Mailand N, Falck J, Lukas C et al. Rapid destruction of human Cdc25A in response to DNA damage. *Science* 2000;288:1425-1429.
28. Dudley DT, Pang L, Decker SJ et al. A synthetic inhibitor of the mitogen-activated protein kinase cascade. *Proc Natl Acad Sci U S A* 1995;92:7686-7689.
29. Favata MF, Horiuchi KY, Manos EJ et al. Identification of a novel inhibitor of mitogen-activated protein kinase kinase. *J Biol Chem* 1998;273:18623-18632.
30. Mummery CL, van den Brink CE, de Laat SW. Commitment to differentiation induced by retinoic acid in P19 embryonal carcinoma cells is cell cycle dependent. *Dev Biol* 1987;121:10-19.
31. Bartek J, Lukas J. Pathways governing G1/S transition and their response to DNA damage. *FEBS Lett* 2001;490:117-122.
32. Lin T, Chao C, Saito S et al. p53 induces differentiation of mouse embryonic stem cells by suppressing Nanog expression. *Nat Cell Biol* 2005;7:165-171.
33. Burdon T, Chambers I, Stracey C et al. Signaling mechanisms regulating self-renewal and differentiation of pluripotent embryonic stem cells. *Cells Tissues Organs* 1999;165:131-143.
34. Buehr M, Smith A. Genesis of embryonic stem cells. *Philos Trans R Soc Lond B Biol Sci* 2003;358:1397-1402; discussion 1402.
35. Mac Auley A, Werb Z, Mirkes PE. Characterization of the unusually rapid cell cycles during rat gastrulation. *Development* 1993;117:873-883.

36. Kranenburg O, de Groot RP, Van der Eb AJ et al. Differentiation of P19 EC cells leads to differential modulation of cyclin-dependent kinase activities and to changes in the cell cycle profile. *Oncogene* 1995;10:87-95.
37. Mummery CL, van Rooijen MA, van den Brink SE et al. Cell cycle analysis during retinoic acid induced differentiation of a human embryonal carcinoma-derived cell line. *Cell Differ* 1987;20:153-160.
38. Resnick JL, Bixler LS, Cheng L et al. Long-term proliferation of mouse primordial germ cells in culture. *Nature* 359:550-551.

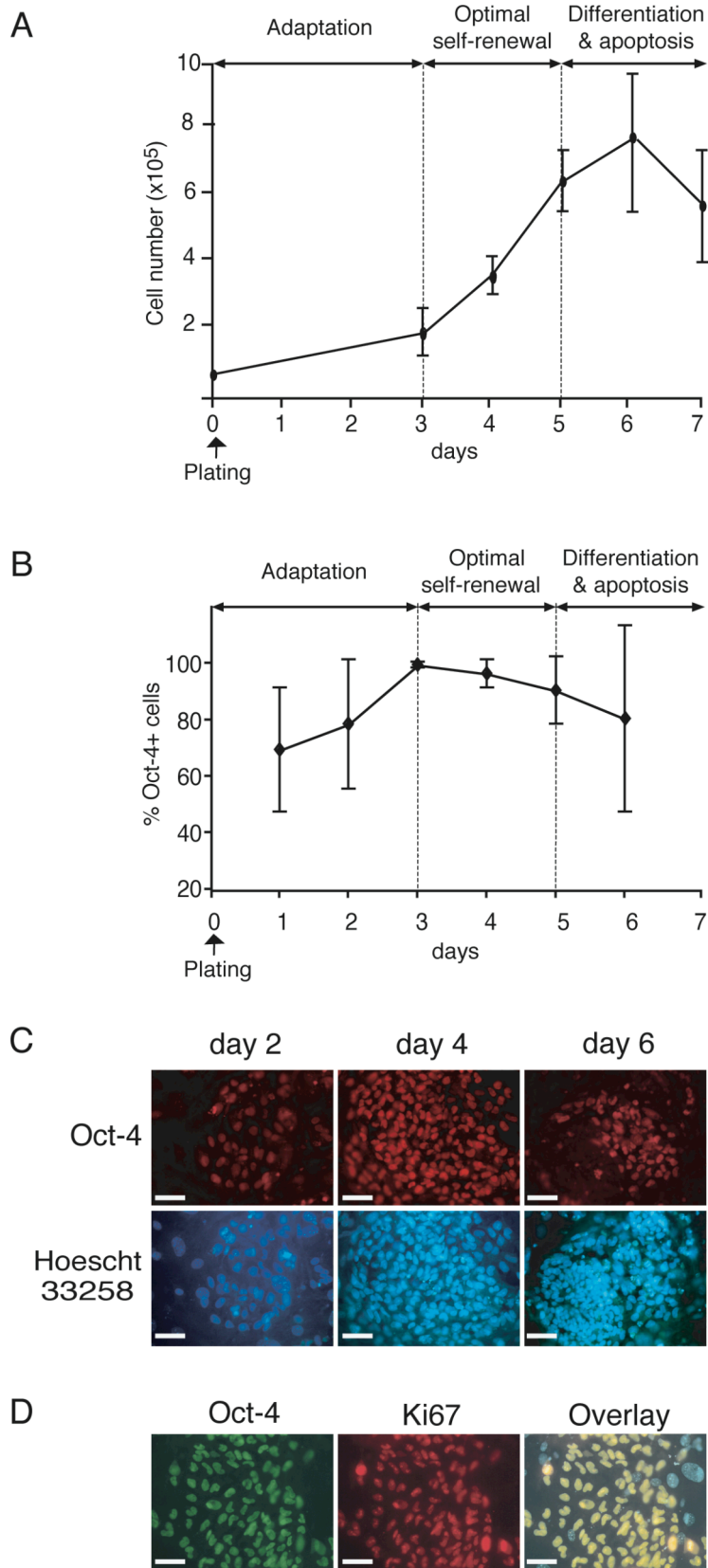


Figure 1

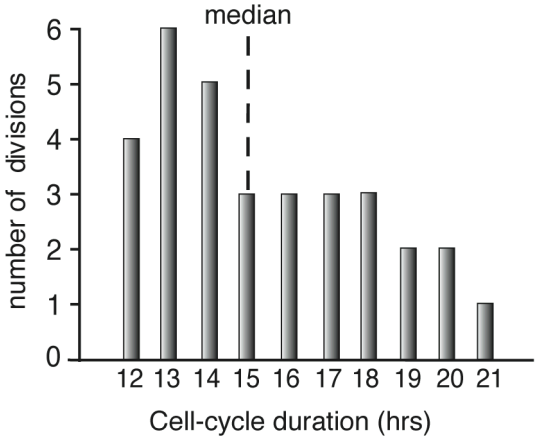


Figure 2

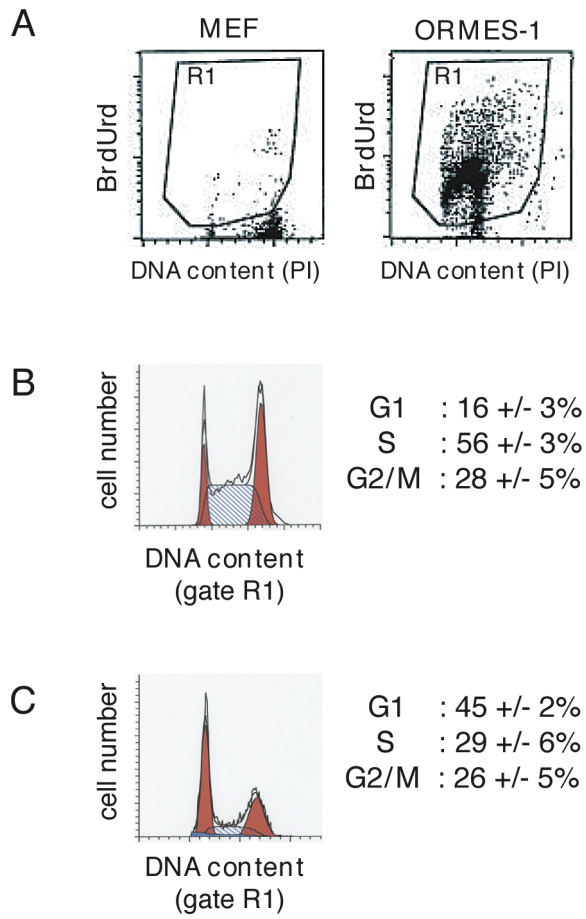


Figure 3

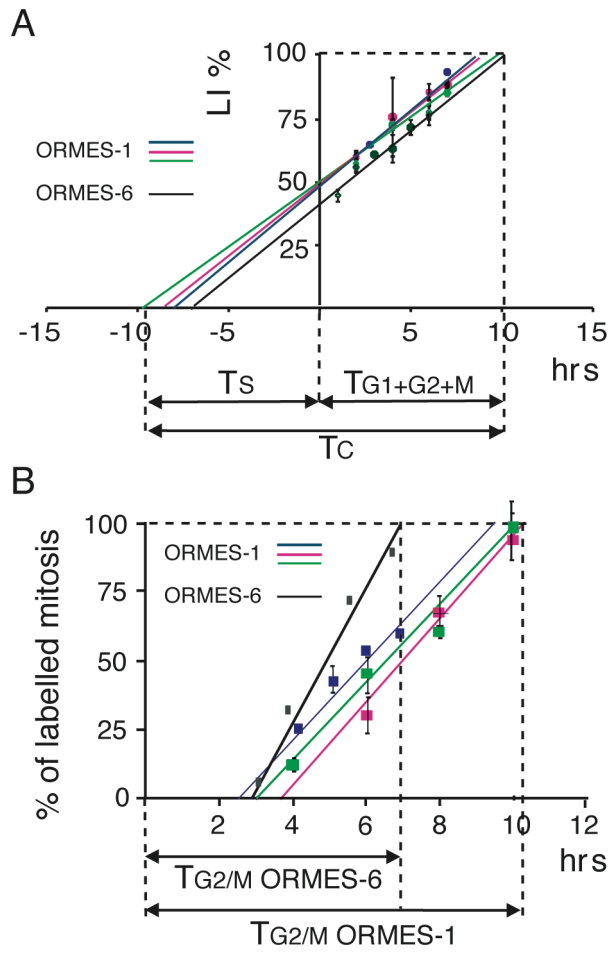


Figure 4

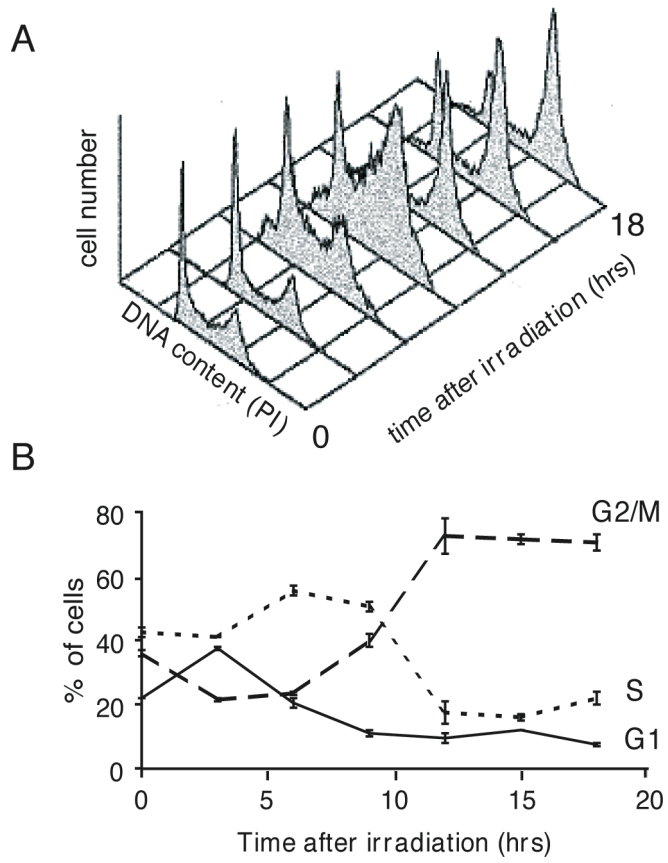


Figure 5

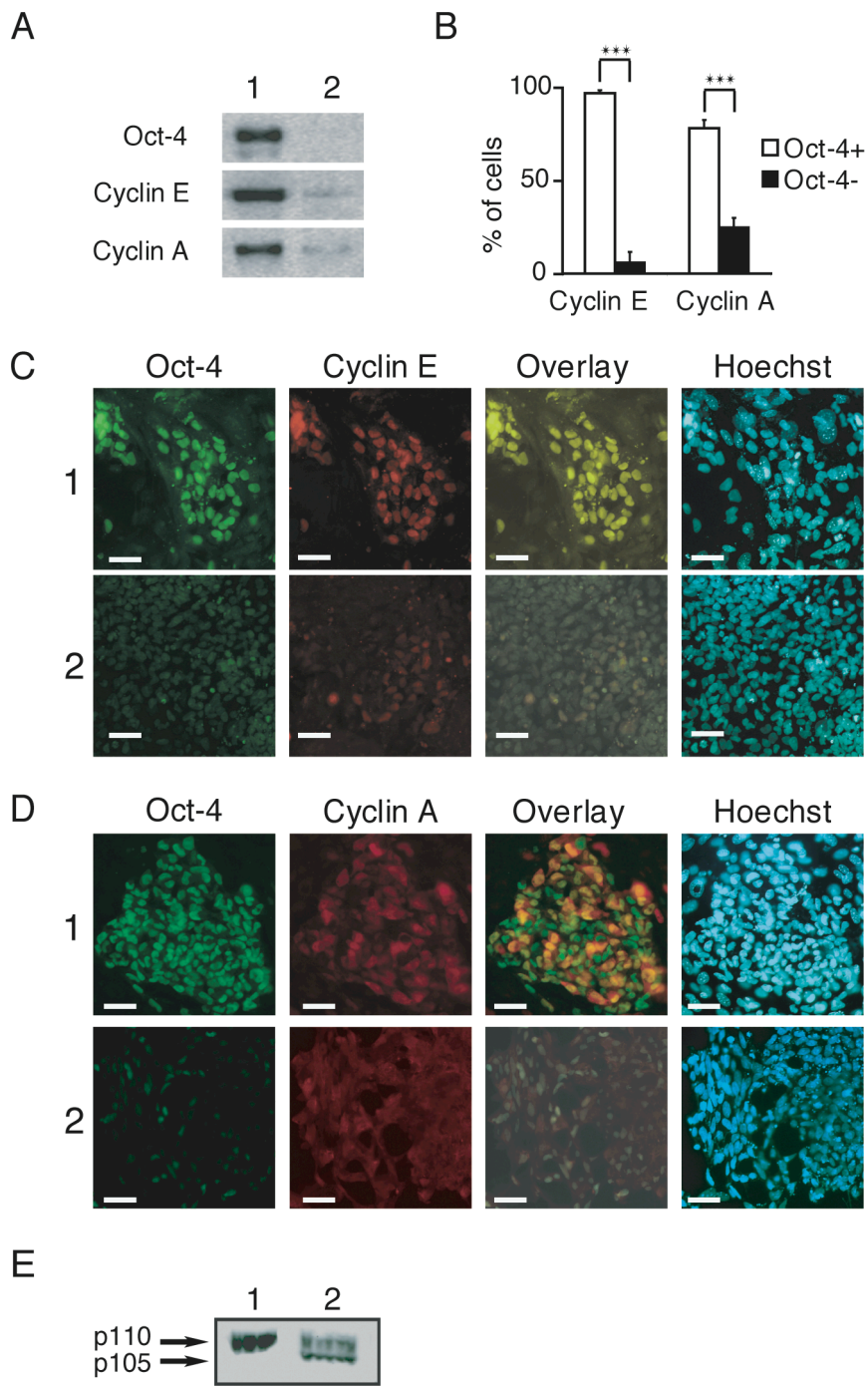


Figure 6

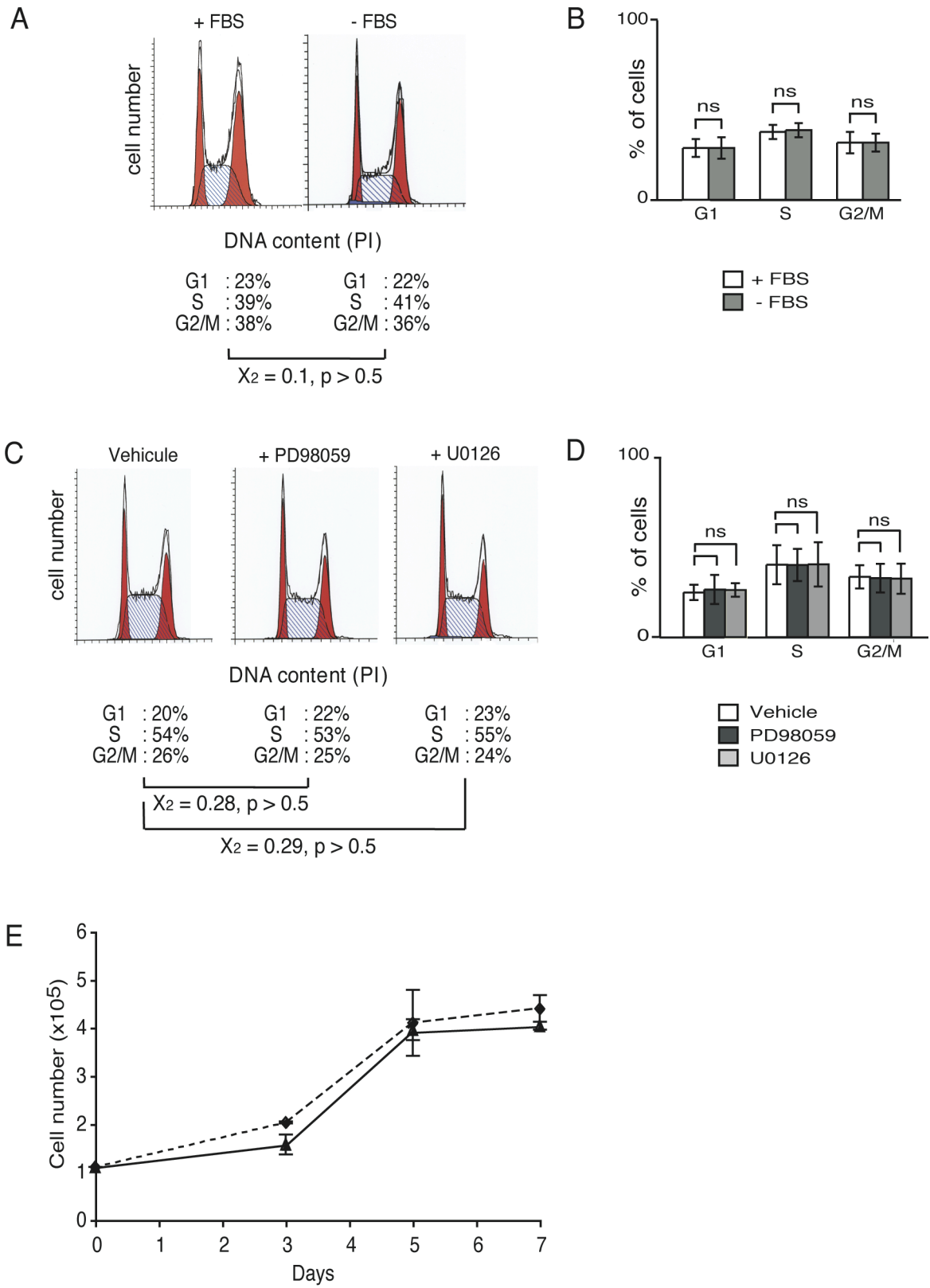


Figure 7